Analysis of Chaotic Circuit Using One Nonlinear Resistor and Two Resonators

Tomohiro Okubo
Dept. Information Science,
Shikoku University
Email: shikoku2003002@yahoo.co.jp

Yasuteru Hosokawa
Dept. Information Science,
Shikoku University
Email: hosokawa@keiei.shikoku-u.ac.jp

Yoshifumi Nishio
Dept. Electrical and Electronic Eng.,
Tokushima University
Email: nishio@ee.tokushima-u.ac.jp

***Abstract*— Until now, we have proposed some chaotic circuits using our designing method. In this study, by using our designing method, a new chaotic circuit is proposed and a generation of chaos is confirmed.**

I. Introduction

Studies of designing principles of chaotic circuits aim to understand chaos and to apply chaos[1]-[12]. Because electric circuit is superior in its simplicity, repeatability and response in the experiment, a electric circuit is a very useful tool for understanding chaos. On the other hand, many researchers developing chaotic circuit applications use a few popular chaotic circuits. In order to develop the excellent application, a chaotic circuit which has suitable characteristics should be used for the application. Therefore, designing methods which can design many kind of chaotic circuits are needed.

In our previous studies, a designing method of chaotic circuits was proposed. This method is to couple an oscillator and a resonator with diodes. In this method, an active element and a nonlinear element is divided. Therefore, a method using one element which combine an active element and a nonlinear element is considered. This idea is already mentioned[12]. However, one chaotic circuit is proposed only and this circuit is not investigated in detail.

In this study, in order to confirm a chaos generation of the circuit, we investigate the circuit in detail.

II. Circuit Model

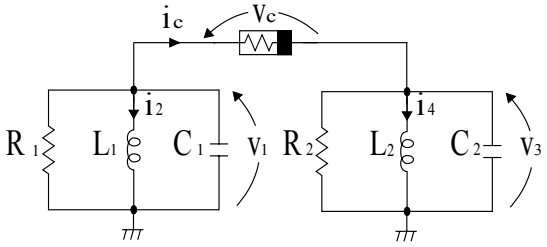

Fig. 1. Chaotic circuit using one nonlinear resistor and two resonators.

Figure 1 shows a chaotic circuit using one nonlinear resistor and two resonators. This circuit is designed based on a following idea.

We have proposed designing method as shown in Fig. 2(a). In this method, one oscillator and one resonator are coupled by diodes. Namely, this system consists of two resonator, one active element and one nonlinear passive element. By combining one active element and one nonlinear passive element, new combination can be considered as shown in Fig. 2(b) In order to investigate this conbination, the circuit as shown in Fig. 1 is invesitgated.

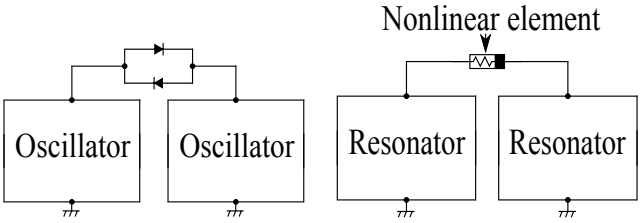

(a) Previous study. (b) This study.

Fig. 2. System models of designing methods of chaotic circuits.

First of all, we derive a simple linearized model of the circuit model in Fig. 1. Figure 3(a) shows the model of a nonlinear element in Fig. 1. The characteristic of this nonlinear element shows a piecewise linear function as shown in Fig. 3(b). The others of circuit elements are modeled as linear elements.

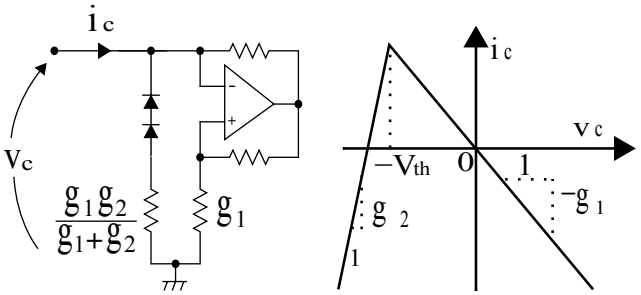

(a) Circuit model. (b) Its characteristic.

Fig. 3. Nonlinear element model.

III. Exact Solutions

By using the linearized circuit model, the circuit equations are derived as follows.

$$\begin{cases} C_1\dfrac{dv_1}{dt} &= -\dfrac{1}{R_1}v_1 - i_2 - i_c, \\ L_1\dfrac{di_2}{dt} &= v_1, \\ C_2\dfrac{dv_3}{dt} &= -\dfrac{1}{R_2}v_3 - i_4 - i_c, \\ L_2\dfrac{di_4}{dt} &= v_3, \end{cases} \tag{1}$$

where,

$$\begin{aligned} i_c = \; & 0.5(g_1+g_2)V_{th} + 0.5(g_2-g_1)v \\ & -0.5(g_1+g_2)|v - V_{th}|. \end{aligned} \tag{2}$$

By changing parameters and variables,

$$\begin{aligned} & x_1 = \frac{v_1}{V_{th}}, \quad x_2 = \sqrt{\frac{L_1}{C_1}}\frac{i_2}{V_{th}}, \quad x_3 = \frac{v_3}{V_{th}}, \\ & x_4 = \sqrt{\frac{L_1}{C_1}}\frac{i_4}{V_{th}}, \quad \alpha_1 = \frac{1}{R_1}\sqrt{\frac{L_1}{C_1}}, \\ & \alpha_2 = \frac{1}{R_2}\sqrt{\frac{L_1}{C_1}}, \quad \beta = g_2\sqrt{\frac{L_1}{C_1}}, \quad \gamma = \frac{C_1}{C_2}, \\ & \delta = \frac{L_1}{L_2}, \quad \varepsilon = \frac{g_1}{g_2}, \quad \tau = \frac{1}{\sqrt{L_1C_1}}t \;\text{ and }\; \frac{d}{dt} = \text{"}\cdot\text{"} \end{aligned} \tag{3}$$

The normalized circuit equations are described by the following four-dimensional piecewise-linear differential equations.

$$\begin{cases} \dot{x}_1 &= -\alpha_1 x_1 - x_2 - \beta y, \\ \dot{x}_2 &= x_1, \\ \dot{x}_3 &= -\gamma(\alpha_2 x_3 + x_4 - \beta y), \\ \dot{x}_4 &= \delta x_3, \end{cases} \tag{4}$$

where,

$$\begin{aligned} y = \; & 0.5(\varepsilon+1) + 0.5(1-\varepsilon)(x_1 - x_3) \\ & -0.5(\varepsilon+1)|x_1 - x_3 + 1|. \end{aligned} \tag{5}$$

Since the circuit equations are piecewise-linear, exact solutions in each linear region can be derived. We define two piecewise-linear regions as follows.

$$\begin{aligned} & \mathbf{R}_1 : x_1 - x_3 + 1 \geq 0, \\ & \mathbf{R}_2 : x_1 - x_3 + 1 < 0, \end{aligned} \tag{6}$$

The eigenvalues in each region can be calculated numerically from Eq. (4). The eigenvalues in each region are described as follows.

$$\begin{aligned} & \mathbf{R}_1 : \sigma_1 \pm j\omega_1, \quad \sigma_2 \pm j\omega_2 \\ & \mathbf{R}_2 : \lambda_1, \quad \lambda_2, \quad \sigma \pm j\omega \end{aligned} \tag{7}$$

Next, we define the equilibrium points in $\mathbf{E}_1$ and $\mathbf{E}_2$ as

$$\mathbf{E}_1 = 0 \quad \text{and} \quad \mathbf{E}_2 = \begin{bmatrix} 0 \\ -\beta(\varepsilon+1) \\ 0 \\ \beta(\varepsilon+1) \end{bmatrix}, \tag{8}$$

respectively. These values are calculated by putting the right side of Eq. (4) to be equal to zero.

Then, we can describe the exact solutions in each linear region as follows.

Region $\mathbf{R_1}$

$$\begin{aligned} & \mathbf{x}(\tau) = \mathbf{F}(\tau)\cdot\mathbf{F}^{-1}(0)\cdot\mathbf{x}(0), \\ & \mathbf{x}(\tau) = \begin{bmatrix} x_1(\tau) \\ x_2(\tau) \\ x_3(\tau) \\ x_4(\tau) \end{bmatrix}, \quad \mathbf{F}(\tau) = \begin{bmatrix} \mathbf{f}_1(\tau) \\ \mathbf{f}_2(\tau) \\ \mathbf{f}_3(\tau) \\ \mathbf{f}_4(\tau) \end{bmatrix}, \\ & \mathbf{f}_2(\tau) = \begin{bmatrix} \mathrm{e}^{\sigma_1\tau}\cos\omega_1\tau \\ \mathrm{e}^{\sigma_1\tau}\sin\omega_1\tau \\ \mathrm{e}^{\sigma_2\tau}\cos\omega_2\tau \\ \mathrm{e}^{\sigma_2\tau}\sin\omega_2\tau \end{bmatrix}, \\ & \mathbf{f}_1(\tau) = \frac{d\mathbf{f}_2}{d\tau}, \quad \mathbf{f}_3(\tau) = \cdots, \quad \mathbf{f}_4(\tau) = \cdots, \end{aligned} \tag{9}$$

Region $\mathbf{R}_2$

$$\begin{aligned} & \mathbf{x}(\tau) - \mathbf{E}_2 = \mathbf{G}(\tau)\cdot\mathbf{G}^{-1}(0)\cdot(\mathbf{x}(0) - \mathbf{E}_2), \\ & \mathbf{x}(\tau) = \begin{bmatrix} x_1(\tau) \\ x_2(\tau) \\ x_3(\tau) \\ x_4(\tau) \end{bmatrix}, \quad \mathbf{G}(\tau) = \begin{bmatrix} \mathbf{g}_1(\tau) \\ \mathbf{g}_2(\tau) \\ \mathbf{g}_3(\tau) \\ \mathbf{g}_4(\tau) \end{bmatrix}, \\ & \mathbf{g_2}(\tau) = \begin{bmatrix} \mathrm{e}^{\lambda_1\tau} \\ \mathrm{e}^{\lambda_1\tau} \\ \mathrm{e}^{\sigma\tau}\cos\omega\tau \\ \mathrm{e}^{\sigma\tau}\sin\omega\tau \end{bmatrix}, \\ & \mathbf{g}_1(\tau) = \frac{d\mathbf{g}_2}{d\tau}, \quad \mathbf{g}_3(\tau) = \cdots, \quad \mathbf{g}_4(\tau) = \cdots, \end{aligned} \tag{10}$$

We omit the descriptions of $\mathbf{f}_k$ and $\mathbf{g}_k$ $(k = 3, 4)$.

IV. Poincaré Map

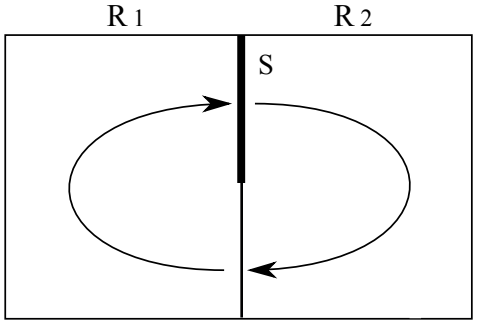

Fig. 4. Derivation of the Poincaré map.

In order to confirm the generation of chaos, we derive the Poincaré map.

Let us define the following subspace

$$\mathbf{S} = \mathbf{S}_1 \cap \mathbf{S}_2 \tag{11}$$

where

$$\begin{aligned} &\mathbf{S}_1 : x_1 - x_3 + 1 = 0 \\ &\mathbf{S}_2 : (-\alpha_1 + \alpha_2\gamma)x_1 - x_2 + \gamma x_4 + \alpha_2\gamma - \beta\varepsilon - \beta\gamma\varepsilon < 0 \end{aligned} \tag{12}$$

The subspace $\mathbf{S}_1$ corresponds to the boundary condition between $\mathbf{R}_1$ and $\mathbf{R}_2$, while the subspace $\mathbf{S}_2$ corresponds to the condition $\dot{x}_1 - \dot{x}_3 < 0$. Namely, $\mathbf{S}$ corresponds to the transitional condition from $\mathbf{R}_1$ to $\mathbf{R}_2$

Let us consider the solution starting from an initial point on $\mathbf{S}$. The solution returns back to $\mathbf{S}$ again after wandering R_2 and R_1 as shown in Fig. 4. Hence, we can derive the Poincaré map as follows.

$$\mathbf{T} : \mathbf{S} \to \mathbf{S}, \quad \mathbf{x}_0 \mapsto \mathbf{T}(\mathbf{x}_0) \tag{13}$$

where $\mathbf{x}_0$ is an initial point on $\mathbf{S}$, while $\mathbf{T}(\mathbf{x}_0)$ is the point at which the solution starting from x_0 hits $\mathbf{S}$ again.

The concrete representation of $\mathbf{T}(\mathbf{x}_0)$ is given as follows using the exact solutions in Eqs. (9) and (10).

Suppose that the solution starting from $\mathbf{x}_0 = (X_{10}, X_{20}, X_{30}, X_{40})$ when $\tau = 0$ hits $\mathbf{S}_1$ and enters $\mathbf{R}_1$ at $\mathbf{x}_1 = (X_{11}, X_{21}, X_{31}, X_{41})$ when $\tau = \tau_1$. In this case, $\mathbf{x}_1$ is given by

$$\begin{bmatrix} X_{11} \\ X_{21} + \beta(\varepsilon + 1) \\ X_{11} + 1 \\ X_{41} - \beta(\varepsilon + 1) \end{bmatrix} = \mathbf{G}(\tau_1) \cdot \mathbf{G}^{-1}(0) \cdot \begin{bmatrix} X_{10} \\ X_{20} + \beta(\varepsilon + 1) \\ X_{10} + 1 \\ X_{40} - \beta(\varepsilon + 1) \end{bmatrix} \tag{14}$$

where τ_1 is given by using the first and third rows of Eq. (14). The solution hits $\mathbf{S}$ again at $\mathbf{x}_2 = (X_{12}, X_{22}, X_{32}, X_{42})$ when $\tau = \tau_1 + \tau_2$. $\mathbf{x}_2$ is given by

$$\begin{bmatrix} X_{12} \\ X_{22} \\ X_{12} + 1 \\ X_{42} \end{bmatrix} = \mathbf{F}(\tau_1) \cdot \mathbf{F}^{-1}(\mathbf{0}) \cdot \begin{bmatrix} X_{11} \\ X_{21} \\ X_{11} + 1 \\ X_{41} \end{bmatrix} \tag{15}$$

where τ_2 is given by using the first and third rows of Eq. (15). Finally, we get

$$\mathbf{T}(\mathbf{x}_0) = \mathbf{x}_2 \tag{16}$$

The jacobian matrix $\mathbf{DT}$ of the Poincaré map $\mathbf{T}$ can be also derived rigorously from Eqs. (14)-(16). We can calculate the largest Lyapunov exponent by

$$\mu = \lim_{N \to \infty} \frac{1}{N} \sum_{j=1}^{N} \log |\mathbf{DT}_j \cdot e_j| \tag{17}$$

where e_j is a normalized base.

Figures 5(1) show circuit experiment results. Horizontal axes are x_1 and vertical axes are x_3. We choose g_1 as the control parameter. Figures 5(2) show computer calculated results of the exact solutions in Eqs. (9) and (10). We choose ε as the control parameter. Figures 5(3) show Poincaré maps

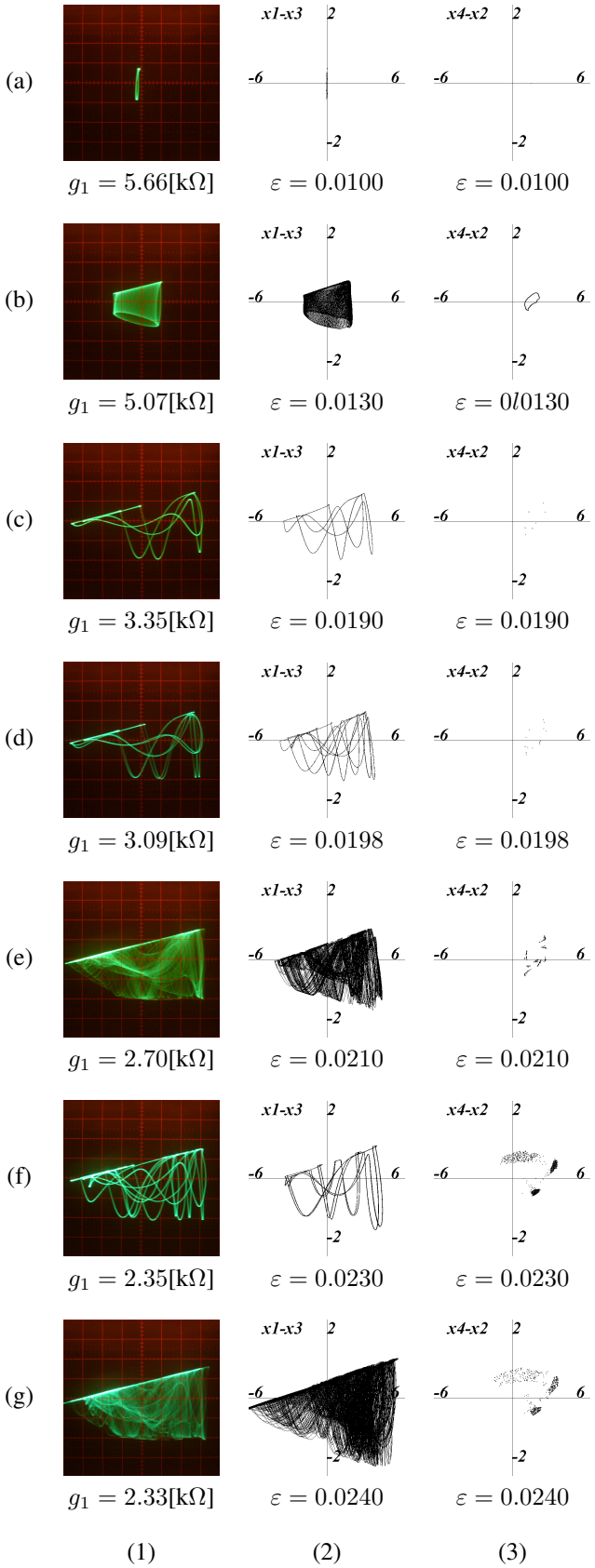

Fig. 5. System models of designing method of chaotic circuits. (1) Circuit Experiments. $R_1 = R_2 = 20.0[\mathrm{k}\Omega]$, $g_2 = 0.0[\Omega]$, $C_1 = 100.0[\mathrm{nF}]$, $C_2 = 10.0[\mathrm{nF}]$, $L_1 = 50.0[\mathrm{mH}]$ and $L_2 = 30.0[\mathrm{mH}]$. (2) Attractors. (3) Poincaré map. $\alpha_1 = 0.05$, $\alpha_2 = 0.05$, $\beta = 9.0$, $\gamma = 10.0$ and $\delta = 1.6$.

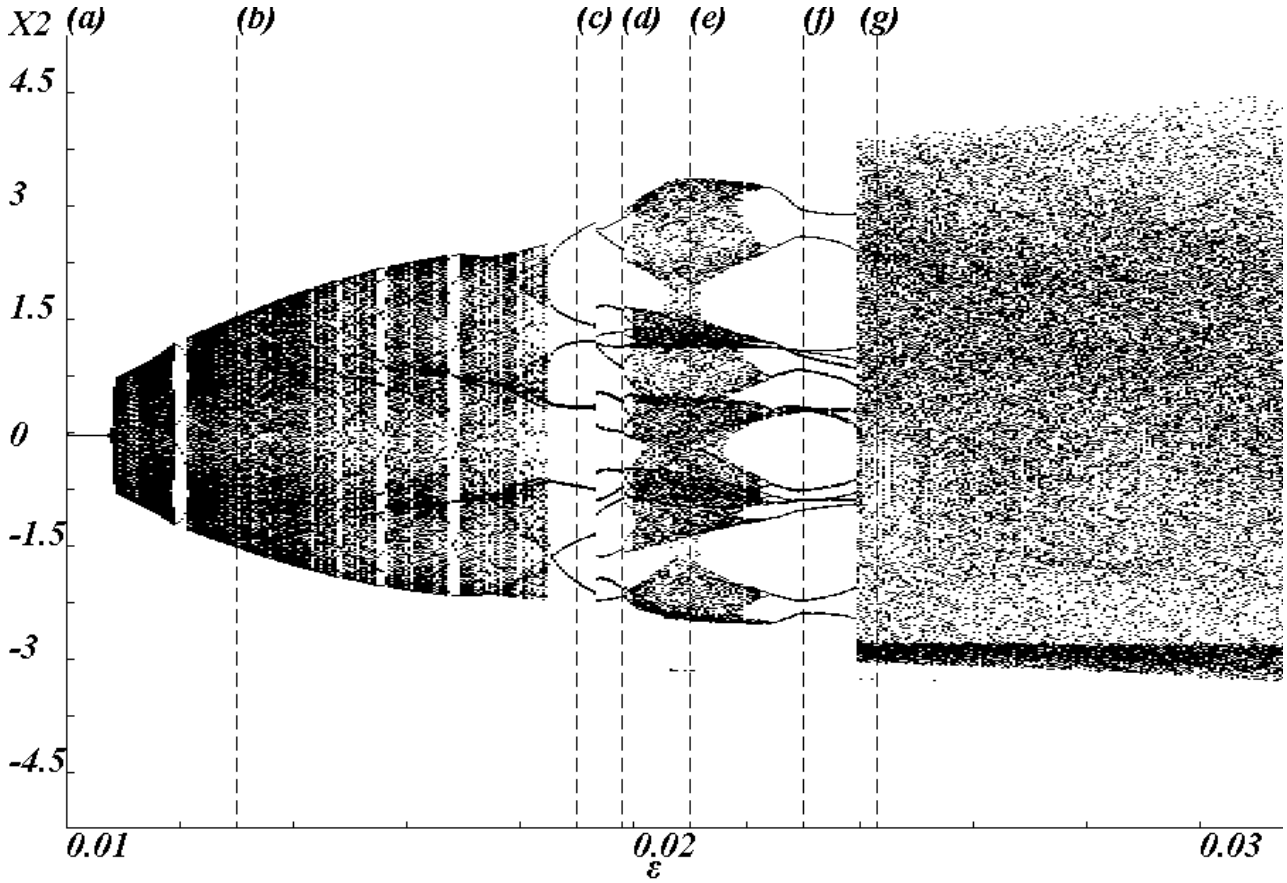

Fig. 6. One-parameter bifurcaition diagram. Horizontal: ε. Vertical: x_2.

obtained by calculating Eqs. (14)-(16). One-parameter bifurcation diagram is shown in Fig. 6. Control parameter is ε and other parameters are fixed as Fig. 5

We can observe almost same attractors and the same bifurcation scenario as follows. In Figs. 5(a), a periodic orbit is observed. By increasing the control parameter, quasi periodic orbit in Figs. 5(b), period-doubling bifurcation in Figs. 5(c)(d) chaos in Figs. 5(e)(g), and window in Figs. 5(f) are observed. We also calculated the largest Lyapunov exponents. In Figs. 5(e) and (g), the value of the largest Lyapunov exponents are $\mu = 0.0958$ and $\mu = 0.1395$, respectively.

V. Conclusions

In this study, we have analyzed a chaotic circuit using one nonlinear resistor and two resonators. we have confirmed the generation of chaos by calculating the largest Lyapunov exponent.

Our future research is the development of a designing method of chaotic circuit based on this study.

References

[1] M. Shinriki M. Yamamoto and S. Mori, "Multimode oscillations in a modified van der Pol Oscillator Containing a Positive Nonlinear Conductance," *Proc. IEEE*, vol. 69, pp. 394–395, 1981.

[2] L. O. Chua, M. Komuro and T. Matsumoto, "The double scroll family," *IEEE Trans. Circuits Syst.*, vol. 33, no. 11, pp. 1073–1118, 1986.

[3] N. Inaba, S. Mori and T. Saito, "Chaotic Phenomena in 3rd Order Autonomous Circuits with a Linear Negative Resistance and an Ideal Diode II," *Technical Report of IEICE*, vol. 87, no. 271, pp. 9-15, 1987.

[4] T. Saito, "An Approach Toward Higher Dimensional Hysteresis Chaos Generators," *IEEE Trans. Circuits Syst.*, vol. 37, No. 3, pp. 399–409, 1990.

[5] J. A. K. Suykens and J. Vandewalle, "Generation of n-double scrolls," *IEEE Trans. Circuits Syst I.*, vol. 40, pp. 861–867, 1993.

[6] M. A. Aziz-Alaoui, "Differential Equations With Multispiral Attractors," *Int. J. Bifurcation & Chaos*, vol. 9, no. 6, pp. 1009–1039, 1999.

[7] Y. Hosokawa, Y. Nishio and A. Ushida, "A Design Method of Chaotic Circuits Using Two Oscillators," *Proc. of NOLTA2000*, vol. 1, pp. 17–21, 2000.

[8] M. Kuramitu and Y. Kurototi, "Generating Chaos through Breaking Symmetry of Limit Cycle (II)," *Technical Report of IEICE*, vol. 100, no. 680, pp.87-94, 2001.

[9] M. E. Yalcin, S. Ozoguz, J. A. K. Suykens and J. Vandewalle, "Families of scroll grid attractors," *Int. J. Bifurcation & Chaos*, vol. 12, no. 1, pp. 23–41, 2001.

[10] A. S. Elwakil and M. P. Kennedy, "Construction of Classes of Circuit-Independent Chaotic Oscillators Using Passive-Only Nonlinear Devices," *IEEE Trans. Circuits Syst I.*, vol. 48, no. 3, pp. 289–306, 2001.

[11] S. O. Scanlan, "Synthesis of Piecewise-Linear Chaotic Oscillators With Prescribed Eigenvalues," *IEEE Trans. Circuits Syst I.*, vol. 48, no. 9, pp. 1057–1064, 2001.

[12] Y. Hosokawa, "Design and Analysis of Continuous-Time Chaotic Circuits Including Diodes," *Doctoral Thesis*, Graduate School of Engineering, The University of Tokushima, Japan, 2002.